DOI: 10.1002/chem.200902743

A Highly Charged Ag_6^{4+} Core in a DNA-Encapsulated Silver Nanocluster

Konrad Koszinowski* and Korbinian Ballweg[a]

Dedicated to Dr. Klaus Römer on the occasion of his 70th birthday

Small metal clusters fill the gap between the atomic scale and the metallic state with its distinctive bulk phenomena.[1] Besides being of high fundamental interest, this intermediate character of metal clusters also gives rise to unique and potentially useful electronic, magnetic, and optical properties.[2] To bring these properties to real-world applications, however, the clusters must be stabilized and prevented from spontaneous aggregation and other decomposition reactions. One successful strategy relies on the immobilization of metal clusters on surfaces.[3] Another approach stabilizes the clusters by the attachment of protective ligands.[4] Quite often the same ligands can also serve as templates for the formation of the metal clusters.[4] This favorable situation is realized for a manifold of silver nanoclusters, which are synthesized by the reduction of silver salts in the presence of templates, such as poly(amidoamine) dendrimers,[5] poly(acrylic acid) derivatives,[6] poly(methacrylic acid),[7] peptides,[8] or DNA.[9] The thus formed nanoclusters contain only a few Ag atoms and hence exhibit molecule-like properties,[10] in contrast to the conventional larger nanoparticles, which more closely resemble the metallic state.[11] In particular, the strong fluorescence of silver nanoclusters has attracted significant attention because of its potential practical applications.[5–10] Among the various species investigated so far, silver nanoclusters encapsulated by the single-stranded oligonucleotide dC_{12} arguably constitute the most promising system thanks to their very high photoemission rates and their excellent photostability.[12]

The recent progress in the synthesis of stabilized silver nanoclusters has been much faster than developing an adequate theoretical understanding of their chemical, electronic, and spectral properties. Any advances in these directions are severely hampered by the fact that the sizes of the Ag_n cluster cores are currently not known precisely and that their charge states remain completely undetermined. Without knowledge of both these quantities and, thus, the number of electrons present in the cluster cores, obviously no meaningful theoretical analysis of the chemical or spectral properties of these species is possible. For the dC_{12}-encapsulated silver nanoclusters, mass-spectrometric studies have suggested rather broad distributions of Ag_n cluster sizes, with n ranging from 2 to 7.[13] The presence of multiple clusters was also inferred from the rather complex optical spectra recorded. The UV/Vis absorption spectrum of an aqueous solution of the in situ formed dC_{12}-stabilized silver species shows a narrow maximum of $\lambda_{max} = 440$ nm and smaller peaks at 350, 570, and 650 nm.[13] These bands are all considered indicative of genuine nanoclusters because they are absent from the absorption spectrum of silver nano*particles*, which only displays one broad peak at $\lambda_{max} = 405$ nm.[13] However, it is unknown to which cluster sizes the different absorption bands correspond. The emission spectra of the nanoclusters are complex as well and moreover change with time, in contrast to the absorption spectrum.[13] This time evolution was rationalized by the occurrence of oxidation reactions.[13] Furthermore, a combination of gel-electrophoretic separation and mass spectrometry provided evidence that just clusters with $n = 2$ and/or 3 are the actual fluorescent chromophores.[12] Again, the charge states of these nanoclusters were not addressed.[12]

Clearly, the simultaneous presence of different dC_{12}-encapsulated silver nanoclusters complicates the interpretation of the experimental results, especially in the case of the optical spectra. We found that changing the pH value can substantially simplify the system and take advantage of this situation to characterize the nanoclusters by a combination of UV/Vis absorption spectroscopy and anion-mode electrospray-ionization (ESI) mass spectrometry. In particular, we show that mass spectrometry can be used to determine the charge states of the clusters with high confidence and report the observation of a remarkably high positive charge of an Ag_6 cluster core.

[a] Dr. K. Koszinowski, K. Ballweg
Department Chemie und Biochemie
Ludwig-Maximilians-Universität München
Butenandtstrasse 5–13, 81377 München (Germany)
Fax: (+49) 89-2180-9977658
E-mail: konrad.koszinowski@cup.uni-muenchen.de

Supporting information for this article is available on the WWW under http://dx.doi.org/10.1002/chem.200902743.

We synthesized the nanoclusters by adding sodium borohydride to an aqueous solution of silver nitrate and the dC_{12} oligonucleotide under air,[14] as described in the literature.[13] The formation of the nanoclusters during the reduction step was evident from the appearance of a yellow color. The UV/Vis absorption spectrum[15] of the solution showed bands at 330, 445, 550, and 645 nm (Figure 1), which indeed closely agree with those reported for dC_{12}-encapsulated Ag_n nanoclusters in the literature (see above).[13]

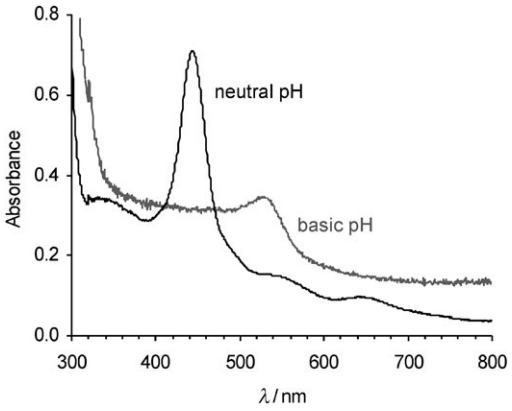

Figure 1. UV/Vis absorption spectra of an aqueous solution of $AgNO_3$/dC_{12}/$NaBH_4$ (ratio 10:1:10, $c(AgNO_3) = 200$ μM) without (black) and with (gray, scaled by a factor of 5) the addition of a mixture of piperidine/imidazole in CH_3CN (c(piperidine) = c(imidazole) = 25 mM relative to the overall solution).

The thus produced solutions were then further analyzed by ESI mass spectrometry. We decided to probe the nanoclusters in the anion mode for the following reasons: i) At neutral and basic pH values, DNA forms polyanions. This anionic character presumably is essential for the suitability of DNA as a template that can bind to Ag^+ ions and it might also be important for stabilizing possibly formed cationic Ag_n nanoclusters. Anion-mode ESI preserves the polyanionic character of the dC_{12} oligonucleotide, whereas cation-mode ESI leads to unnatural protonation states, which might destabilize the Ag_n nanoclusters. ii) The ESI process inherently involves redox reactions.[16] Usually these redox reactions do not affect the ions probed because just ions of the opposite polarity are reduced or oxidized, respectively, at the ESI capillary. However, for redox-sensitive analytes the situation might be different. Thus, it seems possible that cation-mode ESI could oxidize neutral Ag_n nanoclusters, leading to the artifactual detection of cationic nanoclusters. Anion-mode ESI is much less likely to change the oxidation state of neutral Ag_n nanoclusters although it could in turn result in the reduction of cationic Ag_n species. In this case, however, the occurrence of such artifactual reductions should be noticeable by probing simple $AgNO_3$/dC_{12} solutions (without added $NaBH_4$), which form a clear-cut reference of Ag^I.

To facilitate desolvation during the ESI process and achieve good and stable anion signal intensities, the aqueous solutions of the dC_{12}-encapsulated Ag_n nanoclusters were mixed in a ratio of 1:1 with acetonitrile. The addition of CH_3CN did not change the UV/Vis absorption spectrum (see Figure S1 in the Supporting Information) and thus supposedly does not affect the Ag_n nanoclusters. The anion-mode ESI mass spectra obtained for solutions of the nanoclusters showed a multitude of peaks with equal spacings between neighboring m/z values (see Figure S2 in the Supporting Information), which point to extensive adduct formation but do not permit a straightforward assignment. The propensity of DNA polyanions to form adducts with cations is well known[17] and quite expected in the present experiments, which sampled solutions with an excess of Na^+ and Ag^+ salts relative to the dC_{12} oligonucleotide.

An established method to improve anion-mode ESI signal intensities of oligonucleotides and obtain cleaner ESI mass spectra employs basic additives.[18] We therefore mixed the aqueous solution of the dC_{12}-encapsulated nanoclusters with a solution of piperidine/imidazole (c(piperidine) = c(imidazole) = 50 mM) in CH_3CN in a ratio of 1:1, thus shifting the pH value to approximately 12. We noted that upon mixing, the yellow color disappeared to give way to a very faint reddish color. In line with this finding, the UV/Vis absorption spectrum of the basic solution only exhibited a single maximum at 530 nm (Figure 1), which possibly corresponds to the slightly shifted band observed at 550 nm for the neutral solution. The disappearance of the other peaks suggests that the corresponding nanoclusters are no longer stable at high pH values. Presumably, the deprotonation of further sites in the DNA strand and the resulting buildup of negative charge lead to the unfolding of the dC_{12} oligonucleotides, which thus can no longer accommodate the Ag_n cluster cores. In contrast, the persistence of the nanocluster giving rise to the absorption at 530 nm might indicate its particular stability that prevents its decomposition.

We then analyzed the basic solutions of the nanoclusters by anion-mode ESI mass spectrometry.[19] The resulting spectra are no longer congested with excessive adduct peaks but clearly show fourfold deprotonated dC_{12} as the anion with highest signal intensity (Figure 2, top). In addition, tetraanionic complexes of dC_{12} and $n = 3$–8 Ag atoms are discernible, of which the $dC_{12}{\cdot}Ag_6$ species is distinguished by its significantly enhanced intensity. We compared this spectrum with that obtained for a solution of $AgNO_3$ and dC_{12} (containing imidazole/piperidine in CH_3CN) *without* the addition of $NaBH_4$. Without the reduction step, the mass spectrum again indicates the presence of adducts $dC_{12}{\cdot}Ag_n$, $n = 3$–8. However, the maximum of the unimodal intensity distribution now lies at $n = 5$ and no anomalously high signal intensity for $n = 6$ is observed (Figure 2, bottom).

We briefly investigated how the intensity distribution of the $dC_{12}{\cdot}Ag_n$ adducts detected for the solutions of the nanoclusters depended on the $AgNO_3$/dC_{12} ratio. Both for a ratio of 6:1 and 20:1, we also found enhanced intensities for $dC_{12}{\cdot}Ag_6$ after reduction, although this feature was less consistent for the lower ratio. We interpret this preferential formation of $dC_{12}{\cdot}Ag_6$ as an indication of a particular stability

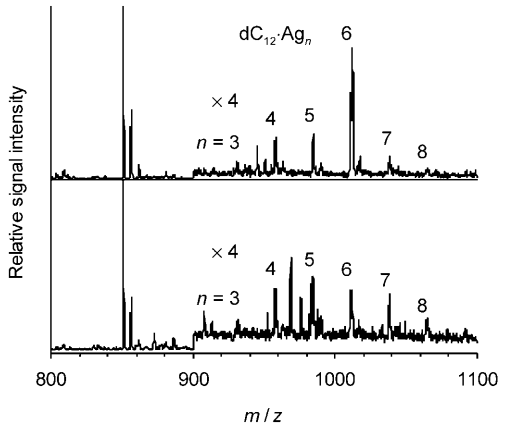

Figure 2. Anion-mode ESI mass spectra of a solution of $AgNO_3/dC_{12}$ (top) after and (bottom) before the addition of $NaBH_4$ (ratio $AgNO_3$/dC_{12}/$NaBH_4$: 10:1:10, $c(AgNO_3)=30\,\mu M$, solvent: water/CH_3CN 1:1 containing piperidine/imidazole, c(piperidine)$=c$(imidazole)$=25$ mM). The base peaks at m/z 851 correspond to the fourfold deprotonated oligonucleotide dC_{12}^{4-}, the neighboring peaks at m/z 856.5 and 862 to Na^+ adducts. At higher m/z ratios, silver adducts $dC_{12}\cdot Ag_n$ are visible. Note that the signal intensities in the range $900 \le m/z \le 1100$ are scaled by a factor of 4.

of a nanocluster with a core of six Ag atoms. Moreover, we correlate this $dC_{12}\cdot Ag_6$ nanocluster with the species that displayed the single absorption band at 530 nm in the UV/Vis spectrum of the nanocluster solution at pH $\approx$ 12.

Next, we analyzed the charge states of the silver atoms in the $dC_{12}\cdot Ag_n$ adducts on the basis of their overall charge and their exact elemental composition. In doing so, we assumed that the dC_{12} oligonucleotide itself does not undergo any redox reactions (see below) but is affected in its charge exclusively by protonation/deprotonation and H^+/Ag^+ exchange reactions. For example, if the addition of one Ag atom to the dC_{12} oligonucleotide is accompanied by the loss of one H atom without a change in the overall charge state, this process corresponds to an H^+/Ag^+ exchange, implying the presence of Ag^+. In contrast, if the number of H atoms remains constant, the presence of Ag^0 follows necessarily. Of course, the main challenge of this approach is to measure the m/z ratios of the $dC_{12}\cdot Ag_n$ adducts with sufficiently high accuracy and resolution such that their elemental compositions can be derived with high confidence.

For our experiments, we used an HCT ion trap instrument (Bruker Daltonik).[19] This quadrupole ion trap does not achieve the high mass resolving power of Fourier-transform ion-cyclotron resonance, Orbitrap, sector-field, or modern time-of-flight mass spectrometers. Nevertheless, it succeeded in partially resolving the isotope pattern of fourfold deprotonated dC_{12} (see Figure S3 in the Supporting Information). The exact identity of this peak was confirmed by high-resolution mass spectrometry (LTQ FT-ICR, Thermo Finnigan), which also proves the absence of artifactual redox reactions of the DNA ligand during the ESI process. We compared the measured isotope pattern with the theoretically predicted one (see Figure S3 in the Supporting Information). The simulation is based on the calculated isotope pattern for $C_{108}H_{141}N_{36}O_{70}P_{11}^{4-}$ and takes into account the exact masses of the isotopes (accuracy of 0.01 amu for the mass of neutral dC_{12} with its elemental composition of $C_{108}H_{145}N_{36}O_{70}P_{11}$).[20] Each peak of the calculated isotope pattern then is convoluted with a Gaussian function of the same width and scaled to match the measured intensity distribution. Apart from the width of the Gaussian function, the scaling factor, and an offset to account for the background intensity, no other fitting parameters are used. In particular, the simulated isotope pattern is *not* shifted laterally to match the measured intensity distribution. The good agreement observed (see Figure S3 in the Supporting Information) proves that the HCT ion trap is well-suited for determining the elemental composition of heavy, polycharged species. In all further cases, we used the peak of the fourfold deprotonated dC_{12} anion as an internal reference to check the calibration of the instrument. Only mass spectra with an agreement between measured and predicted isotope pattern comparable to that of Figure S3 in the Supporting Information were considered for the analysis of the $dC_{12}\cdot Ag_n$ peaks.[21]

We then analyzed the elemental compositions of fourfold negatively charged $dC_{12}\cdot Ag_n$ adducts, $n=4$–6, formed *without* addition of $NaBH_4$. These species should contain only Ag^+ unless the ESI process led to artifactual reduction reactions (see above). The comparison of the measured spectra with the simulated isotope patterns for simple $(Ag^+)_n$ adducts showed a reasonably good agreement in all three cases (see Figure S4 and S5 in the Supporting Information for $n=4$ and 5, respectively, and Figure 3 for $n=6$; for $n=5$, the agreement is somewhat impaired by the rather low signal intensity and the relatively poor signal/noise ratio). This consistency excludes the occurrence of interfering redox reactions during the ESI process and lends further support to the validity of our approach.

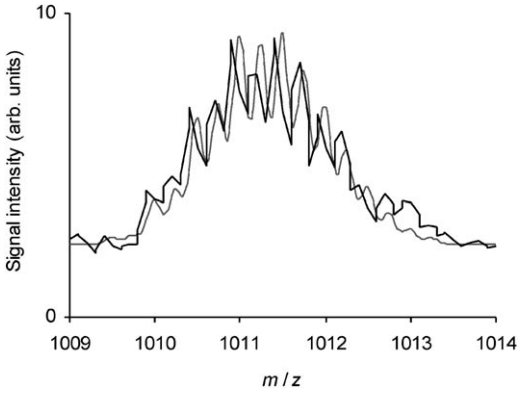

Figure 3. Section from the anion-mode ESI mass spectrum of a solution of $AgNO_3/dC_{12}$ (black) together with the simulated isotope pattern for $C_{108}H_{135}Ag_6N_{36}O_{70}P_{11}^{4-}$ corresponding to $dC_{12}^{10-}\cdot(Ag^+)_6$ (gray).

We then turned to the silver adducts formed *after* the addition of $NaBH_4$. For the tetraanions of $dC_{12}\cdot Ag_n$, $n=4$ and 5, we found elemental compositions indicative of simple $(Ag^+)_n$ adducts (see Figure S6 and S7 in the Supporting In-

formation). These species thus do not correspond to nanoclusters. In contrast, the measured isotope pattern of the fourfold negatively charged $dC_{12}{\cdot}Ag_6$ adduct is reproduced only very poorly by the simulation if a $dC_{12}^{10-}{\cdot}(Ag^+)_6$ species is assumed (see Figure S8 in the Supporting Information). The measured spectrum is shifted toward heavier masses, implying that it contains a higher number of protons than taken into account in the simulation. This means that the $dC_{12}{\cdot}Ag_6$ adduct contains Ag atoms in reduced oxidation states and thus corresponds to a genuine nanocluster.

We then compared the measured spectrum with the simulated isotope patterns of $dC_{12}^{9-}{\cdot}Ag_6^{5+}$, $dC_{12}^{8-}{\cdot}Ag_6^{4+}$, and $dC_{12}^{7-}{\cdot}Ag_6^{3+}$ (see Figures S9–S11, respectively, in the Supporting Information) and found best agreement for $dC_{12}^{8-}{\cdot}Ag_6^{4+}$ (see Figure S10). A careful inspection reveals, however, that the measured isotope pattern is shifted very slightly toward lower masses relative to the simulation. This small deviation might hardly be considered significant were it not the case that we found it consistently in several independent experiments. Moreover, the deviation was more pronounced for those experiments, in which the relative enhancement of $dC_{12}^{8-}{\cdot}Ag_6^{4+}$ compared to the simple $(Ag^+)_n$ adducts was somewhat smaller than usually. We thus reasoned that the deviation might result from the presence of a small amount of unreduced $dC_{12}^{10-}{\cdot}(Ag^+)_6$ besides the $dC_{12}^{8-}{\cdot}Ag_6^{4+}$ nanocluster. We approximated the relative abundance of the former by linearly interpolating the signal intensities of $dC_{12}^{9-}{\cdot}(Ag^+)_5$ and $dC_{12}^{11-}{\cdot}(Ag^+)_7$. Thereby, we arrived at a ratio of approximately 4:1 between the $dC_{12}^{8-}{\cdot}Ag_6^{4+}$ nanocluster and the unreduced $dC_{12}^{10-}{\cdot}(Ag^+)_6$ adduct for the specific measurement shown. A simulation taking into account this ratio indeed reproduced the observed isotope pattern almost perfectly (Figure 4).

We also investigated the $dC_{12}{\cdot}Ag_n$ adducts with a total charge of −5. These experiments were performed with a lower mass resolving power (ultrascan mode) to maximize the signal intensity. Again, we observed the preferential formation of a $dC_{12}{\cdot}Ag_6$ species (see Figure S12 in the Supporting Information). We compared the measured intensity distribution for the pentaanion of $dC_{12}{\cdot}Ag_6$ with the envelopes of the simulated isotope patterns of $dC_{12}^{11-}{\cdot}(Ag^+)_6$, $dC_{12}^{10-}{\cdot}Ag_6^{5+}$, $dC_{12}^{9-}{\cdot}Ag_6^{4+}$, and $dC_{12}^{8-}{\cdot}Ag_6^{3+}$ (see Figure S13–S16, respectively, in the Supporting Information). The best agreement is found for $dC_{12}^{9-}{\cdot}Ag_6^{4+}$ (Figure S15), which is even further improved if the presence of a small amount of unreduced $dC_{12}^{11-}{\cdot}(Ag^+)_6$ is accounted for (Figure S17).

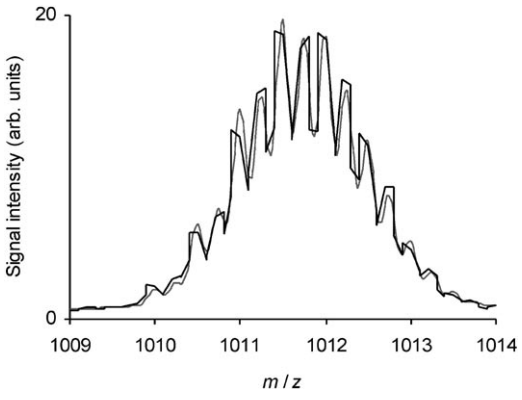

Figure 4. Section from the anion-mode ESI mass spectrum of a solution of $AgNO_3/dC_{12}/NaBH_4$ (black) together with the simulated isotope pattern for a 4:1 mixture of $C_{108}H_{137}Ag_6N_{36}O_{70}P_{11}^{4-}$, corresponding to the nanocluster $dC_{12}^{8-}{\cdot}Ag_6^{4+}$, and $C_{108}H_{135}Ag_6N_{36}O_{70}P_{11}^{4-}$, corresponding to the unreduced adduct $dC_{12}^{10-}{\cdot}(Ag^+)_6$ (gray).

Our results thus consistently point to the preferential formation of nanoclusters that comprise an Ag_6^{4+} core at pH $\approx$ 12. These $dC_{12}{\cdot}Ag_6^{4+}$ nanoclusters presumably do not correspond to the actual fluorescent chromophores, which most likely contain Ag_2 and/or Ag_3 cluster cores.[12] It might seem surprising that the $dC_{12}{\cdot}Ag_6^{4+}$ nanoclusters with their high positive charge are stable toward Coulomb explosion. However, one must not forget that the cluster core is stabilized by the polyanionic DNA ligand, which is supposed to provide significant amounts of negative charge density and balance the high positive charge of the Ag_6^{4+} core in this way (the dC_{12} oligonucleotide has been shown to bind to Ag_n cluster cores via its N3 atoms).[13] The resulting strong interaction between the dC_{12} ligand and the cluster core also explains the stability of this nanocluster at pH $\approx$ 12, whereas clusters with Ag_n cores of lower positive charge densities apparently cannot prevent the multiply deprotonated and highly negatively charged dC_{12} oligonucleotide from unfolding. The UV/Vis absorption spectra furthermore possibly indicate that the $dC_{12}{\cdot}Ag_6^{4+}$ nanocluster does not only form under basic conditions but that it already exists at neutral pH, then giving rise to a slightly shifted absorption at $\lambda_{max}=$ 550 nm. Such a shift in λ_{max} might result from partial protonation of the polyanionic DNA ligand at neutral pH.

Interestingly, an Ag_6^{4+} cluster was previously suggested in a different context, namely as a product of a spontaneous reduction of Ag-exchanged type-A zeolites upon dehydration.[22] Based on X-ray diffraction and reflectance spectroscopy data, Gellens et al. proposed the formation of Ag_3^{2+} at mild conditions, for which they observed a yellow color.[22] Upon evacuation at 300 °C, the color changed to red, which was rationalized by the interaction of two Ag_3^{2+} species to yield Ag_6^{4+}.[22] The correlation of the red color with the Ag_6^{4+} motif strikingly resembles our present results, which associate the absorption band at 530 nm with the $dC_{12}{\cdot}Ag_6^{4+}$ nanocluster. Note, however, that the formation of silver nanoclusters in zeolites by spontaneous reduction has been called into question[23] such that there seems to be no previous undisputed evidence for the observation of Ag_6^{4+} clusters. Notwithstanding, the existence of closely related species formed by radiolytic reductions, such as Ag_3^{2+} and even Ag_4^{3+}, has been established[24] and provides the context in which the stability of the DNA-encapsulated Ag_6^{4+} nanocluster is to be seen.

While our experiments show that dC_{12}-stabilized Ag_6^{4+} is formed after the addition of $NaBH_4$, it remains open whether this species results directly from the reduction of DNA-bound Ag^+ or whether it originates from the oxidation of

previously formed transient nanoclusters in lower oxidation states. Ritchie et al. put forward evidence for the involvement of such intermediate nanoclusters, which are believed to be subsequently oxidized by air.[13] We attempted to identify such putative species in experiments performed under exclusion of air (for the nanocluster synthesis as well as for the ESI mass-spectrometric measurements). However, we found only very low yields of $dC_{12}{\cdot}Ag_n$ adducts and the analysis of the elemental composition for the tetraanion of $dC_{12}{\cdot}Ag_6$ did not reveal a lower oxidation state than that observed in the experiments under aerobic conditions (see Figure S18 in the Supporting Information).

Finally, we briefly investigated how varying the length of the oligonucleotide template affected the formation of DNA-stabilized Ag_n nanoclusters. Using dC_6 as template, we observed a rather broad band in the UV/Vis spectrum of the $AgNO_3/dC_6/NaBH_4$ solution at neutral pH ($\lambda_{max}=$ 440 nm, see Figure S19 in the Supporting Information) and could not detect any $dC_6{\cdot}Ag_n$ adducts by anion-mode ESI mass spectrometry of the solution at pH $\approx$ 12. In contrast, a solution of $AgNO_3/dC_{18}/NaBH_4$ displayed a narrow band at $\lambda_{max}=440$ nm under neutral conditions and thus clearly indicated the formation of $dC_{18}{\cdot}Ag_n$ nanoclusters (see Figure S20 in the Supporting Information). ESI mass-spectrometric analysis of the solution at pH $\approx$ 12 showed the presence of $dC_{18}{\cdot}Ag_n$ adducts. For the determination of the charge states of the Ag atoms, we focused on the pentaanions. The simulated isotope patterns for dC_{18}^{5-} and $dC_{18}^{11-}{\cdot}(Ag^+)_6$ (see Figure S21 and S22, respectively, in the Supporting Information) match the measured intensity distributions of the bare oligonucleotide and the Ag_6 adduct (formed *without* addition of $NaBH_4$) reasonably well. This agreement again demonstrates the accurate calibration of the mass spectrometer and the absence of artifactual redox reactions during the ESI process. The measured isotope distribution of the species formed after the addition of $NaBH_4$ can be satisfactorily fitted if we assume the presence of $dC_{18}^{9-}{\cdot}Ag_6^{4+}$ along with some residual unreduced $dC_{18}^{11-}{\cdot}(Ag^+)_6$ (see Figure S23 in the Supporting Information). Hence, the formation of the Ag_6^{4+} cluster core is apparently not restricted to the use of the dC_{12} oligonucleotide as template although a minimum length of the DNA single strand seems to be essential.

In conclusion, we have shown that the reduction of aqueous $AgNO_3$ in the presence of the oligonucleotide dC_{12} affords nanoclusters with an Ag_6^{4+} core at high pH values. Small silver clusters with comparably high cationic charges have been observed before but not in the context of DNA encapsulation or most other typical template-assisted syntheses. Our findings suggest that such highly charged silver clusters may be more common than thought previously and that the possibility of their presence should be considered for the interpretation of UV/Vis-spectral features. For the $dC_{12}{\cdot}Ag_6^{4+}$ species detected in the present work, the UV/Vis absorption spectrum shows an absorption band of 530 nm (at basic pH). Moreover, we have demonstrated that mass spectrometry can be used to derive the charge states of the metallic cores of encapsulated nanoclusters by the determination of their exact elemental compositions. The experimental derivation of these charge states is the prerequisite for a thorough theoretical understanding of the chemical and spectral properties of metal nanoclusters.

Acknowledgements

We thank Prof. Herbert Mayr and Prof. Thomas Carell for their support and gratefully acknowledge funding from Ludwig-Maximilians-Universität München (LMUexcellent), Deutsche Forschungsgemeinschaft (SFB 749), the Center for Integrated Protein Science Munich, and the Fonds der Chemischen Industrie. K.K thanks the Dr. Klaus Römer-Stiftung for generous additional support.

Keywords: cluster compounds · DNA · mass spectrometry · nanoclusters · silver · UV/Vis spectroscopy

[1] a) W. A. de Heer, *Rev. Mod. Phys.* **1993**, *65*, 611–676; b) M. Brack, *Rev. Mod. Phys.* **1993**, *65*, 677–732; c) *Metal Clusters* (Ed.: W. Ekardt), Wiley, Chichester **1999**.
[2] a) R. Sessoli, D. Gatteschi, A. Caneschi, M. A. Novak, *Nature* **1993**, *365*, 141–143; b) G. Schmid, G. L. Hornyak, *Curr. Opin. Solid State Mater. Sci.* **1997**, *2*, 204–212; c) D. I. Gittins, D. Bethell, D. J. Schiffrin, R. J. Nichols, *Nature* **2000**, *408*, 67–69; d) S. A. Claridge, A. W. Castleman, Jr., S. N. Khanna, C. B. Murray, A. Sen, P. S. Weiss, *ACS Nano* **2009**, *3*, 244–255.
[3] J. Bansmann, S. H. Baker, C. Binns, J. A. Blackman, J.-P. Bucher, J. Dorantes-Dávila, V. Dupuis, L. Favre, D. Kechrakos, A. Kleibert, K.-H. Meiwes-Broer, G. M. Pastor, A. Perez, O. Toulemonde, K. N. Trohidou, J. Tuaillon, Y. Xie, *Surf. Sci. Rep.* **2005**, *56*, 189–275.
[4] G. Schön, U. Simon, *Colloid Polym. Sci.* **1995**, *273*, 101–117.
[5] J. Zheng, R. M. Dickson, *J. Am. Chem. Soc.* **2002**, *124*, 13982–13983.
[6] Z. Shen, H. Duan, H. Frey, *Adv. Mater.* **2007**, *19*, 349–352.
[7] L. Shang, S. Dong, *Chem. Commun.* **2008**, 1088–1090.
[8] J. Yu, S. A. Patel, R. M. Dickson, *Angew. Chem.* **2007**, *119*, 2074–2076; *Angew. Chem. Int. Ed.* **2007**, *46*, 2028–2030.
[9] a) J. T. Petty, J. Zheng, N. V. Hud, R. M. Dickson, *J. Am. Chem. Soc.* **2004**, *126*, 5207–5212; b) C. T. Wirges, J. Timper, M. Fischler, A. S. Sologubenko, J. Mayer, U. Simon, T. Carell, *Angew. Chem.* **2009**, *121*, 225–229; *Angew. Chem. Int. Ed.* **2009**, *48*, 219–223.
[10] T.-H. Lee, J. I. Gonzalez, J. Zheng, R. M. Dickson, *Acc. Chem. Res.* **2005**, *38*, 534–541.
[11] D. D. Evanoff, Jr., G. Chumanov, *ChemPhysChem* **2005**, *6*, 1221–1231.
[12] T. Vosch, Y. Antoku, J.-C. Hsiang, C. I. Richards, J. I. Gonzalez, R. M. Dickson, *Proc. Natl. Acad. Sci. USA* **2007**, *104*, 12616–12621.
[13] C. M. Ritchie, K. R. Johnsen, J. R. Kiser, Y. Antoku, R. M. Dickson, J. T. Petty, *J. Phys. Chem. C* **2007**, *111*, 175–181.
[14] Typical procedure: To an aqueous solution of oligonucleotide dC_{12} (biomers.net, 25 μM, 1.0 mL) cooled to 0 °C, a cold aqueous solution of $AgNO_3$ (180 μM, 1.4 mL) was added. The resulting mixture was immediately combined with a cold aqueous solution of $NaBH_4$ (180 μM, 1.4 mL), vigorously shaken for 2 min, and allowed to age for > 1 h.
[15] UV/Vis absorption spectra were recorded with a Lambda 16 double-beam instrument (Perkin–Elmer).
[16] G. J. Van Berkel, *J. Mass Spectrom.* **2000**, *35*, 773–783.
[17] C. G. Huber, H. Oberacher, *Mass Spectrom. Rev.* **2001**, *20*, 310–343.
[18] N. Potier, A. Van Dorsselaer, Y. Cordier, O. Roch, R. Bischoff, *Nucleic Acids* **1994**, *34*, 3895–3903.

[19] The ESI mass-spectrometric experiments were performed with an HCT ion trap (Bruker Daltonik). Sample solutions were introduced at typical flow rates of 5 $\mu L\,min^{-1}$. Nitrogen was used as sheath gas and an ESI voltage of 3.5 kV was applied. Nitrogen heated to 150 °C was employed as drying gas (5.0 $L\,min^{-1}$). The ions were then transferred into the instrument's three-dimensional quadrupole ion trap filled with helium (Air Liquide, 99.999 % purity, estimated pressure $p(He) \approx 2$ mtorr). The Compass 1.3 software package was used to eject the ions from the trap for their detection. Most of the spectra were acquired in the so-called standard-enhanced mode. For calibration, a standard mixture of substituted phosphazines (Agilent G1969–85000) was employed.

[20] Isotope patterns based on the natural abundances of the elements can be conveniently calculated by web-based resources, such as: http://yanjunhua.tripod.com/pattern.htm.

[21] In some instances, a less satisfactory agreement was observed, the peaks being broader than expected. Presumably, in these cases too many ions were filled into the trap and gave rise to space charges and/or the voltage of the detector was not properly adjusted.

[22] L. R. Gellens, W. J. Mortier, R. A. Schoonheydt, J. B. Uytterhoeven, *J. Phys. Chem.* **1981**, *85*, 2783–2788.

[23] R. Seifert, A. Kunzmann, G. Calzaferri, *Angew. Chem.* **1998**, *110*, 1604–1606; *Angew. Chem. Int. Ed.* **1998**, *37*, 1522–1524.

[24] a) C. E. Forbes, M. C. R. Symons, *Mol. Phys.* **1974**, *27*, 467–471; b) A. Henglein, *Chem. Phys. Lett.* **1989**, *154*, 473–476; c) M. Mostafavi, N. Keghouche, M.-O. Delcourt, *Chem. Phys. Lett.* **1990**, *169*, 81–84; d) A. Henglein, T. Linnert, P. Mulvaney, *Ber. Bunsen-Ges. Phys. Chem.* **1990**, *94*, 1449–1457; e) S. Remita, J. M. Orts, J. M. Feliu, M. Mostafavi, M. O. Delcourt, *Chem. Phys. Lett.* **1994**, *218*, 115–121; f) E. Janata, A. Henglein, B. G. Ershov, *J. Phys. Chem.* **1994**, *98*, 10888–10890; g) B. G. Ershov, A. Henglein, *J. Phys. Chem. B* **1998**, *102*, 10663–10666; h) E. Janata, *J. Phys. Chem. B* **2003**, *107*, 7334–7336.

Received: October 5, 2009
Published online: February 18, 2010

